TELKOMNIKA, Vol.16, No.6, December 2018, pp.2616~2621
ISSN: 1693-6930, accredited First Grade by Kemenristekdikti, Decree No: 21/E/KPT/2018
DOI: 10.12928/TELKOMNIKA.v16i6.9595

Performance Enhancement of Wideband Reflectarray Antennas Embedded on Paper Substrate Materials

M. Y. Ismail*, H. I. Malik
Universiti Tun Hussein Onn Malaysia (UTHM), Parit Raja 86400, Batu Pahat, Johor, Malaysia
*Corresponding author, e-mail: yusofi@uthm.edu.my

Abstract

This research presents an innovative solution to address the bandwidth limitation of microstrip reflectarray antennas. Organic substrate materials with controlled compositions have been characterized to be employed as substrate materials for microstrip reflectarrays. The three proposed materials show low dielectric permittivity values of 1.81, 1.64 and 1.84 along with loss tangents of 0.053, 0.047 and 0.057 respectively. The proposed substrate materials have been verified by modelling reflectarray unit elements in CST MWS and measured using a waveguide simulator technique. The comparison between measured and simulated results show a good agreement with promising broadband performance of 312, 340 and 207 MHz for S1, S2 and S3 substrate materials respectively.

Keywords*: reflectarray antenna; broadband; paper substrate*

1. Introduction

Microstrip reflectarray antennas are a planar class of antennas with one, two or three layered structures fed by a primary source antenna. Due to their compact size, low profile, spatial feeding, they present themselves as an attractive antenna for long range and high gain applications such as radar and space applications [1]. Moreover due to structural simplicity they are highly recommended at microwave and terahertz frequencies [2-4]. The fundamental principle of reflectarray operation is the same as that of a parabolic dish reflector; however the curved paraboloid of dish reflector is replaced by a flat structure with a printed array of radiating elements. The individual phases of the elements are organized in such a manner that compensates the differential phase delay caused by the flat profile of reflectarray antenna [5]. The phase compensation techniques have been reported to be implemented using various element configurations such as stub loaded elements, elements with variable sizes or rotation angles and elements with different slot configurations [6-12]. In all the stated phasing techniques one or two parameters of the radiating element are adjusted to achieve a progressive phase distribution over the array.

Since microstrip reflectarray antennas are derived from microstrip antenna technology, so intrinsically they suffer from narrow bandwidth. For a microstrip patch the bandwidth is limited to 3-5% only [13]. Two different approaches have been reported to address the bandwidth limitation. The first technique consists of using reflectarray elements with wider phase ranges of greater than 360º [14-16]. The second technique is based on the introduction of dual resonance elements with resonances in same or different frequency bands [17-19]. The first stated solution for narrow bandwidth limitation requires multi-layered assembly of flat printed arrays. This increases the fabrication complexity of the design requiring precise arrangement and alignment of the stacked structure. The second solution of using a dual resonance element requires complex phase distribution techniques to acquire fruitful radiation patterns at both resonances.

The research focuses on a novel introduction of innovative paper substrate materials with controlled composition for microstrip reflectarray antenna. Three different substrate materials have been manufactured with controlled composition of recycled materials. The proposed substrates have been characterized for electrical properties. In order to evaluate the performance of microstrip reflectarray antenna based on proposed substrates, unit elements have been simulated and fabricated. The performance of fabricated reflectarray elements on novel substrates have been analysed and compared based on scattering parameter results.

Received April 13, 2018; Revised April 28, 2018; Accepted May 9, 2018

2. Dielectric Material Characterization

The proposed paper substrate materials were derived from banana pulp, recycled newspaper and recycled carton paper. Controlled quantities of these materials were mixed together to achieve low permittivity behaviors. The dielectric materials were first characterized using a broadband characterization technique based on dielectric probe method. Figure 1 shows the proposed paper substrate materials. The three different types of substrate materials are named as S1, S2 and S3 for identification. Figure 2 shows the dielectric material characterization set-up for the paper substrates.

Figure 1. Different types of proposed paper substrate materials

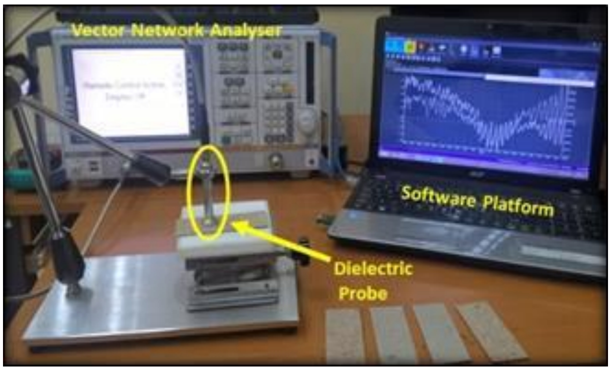

Figure 2. Dielectric material characterization set-up

The characterization set-up for paper substrate material consists of dielectric probe, vector network analyzer (VNA) and a software platform based on PC. The probe was attached to VNA, while the VNA was controlled remotely by the software platform. The whole system was first carefully calibrated with water as a load due to the universal properties of water. A fixture stand was used for adjusting the substrate under test with full contact of probe face. The fixture can be moved in vertical direction thus it was kept at a constant contact position after fixing the probe. The results of material characterization are tabulated in Table 1.

Table 1. Dielectric Material Characterization Results

Substrate	ε_r	tanδ	Height(mm)
S1	1.81	0.053	1.45
S2	1.63	0.046	1.62
S3	1.84	0.057	1.12

Table 1 shows the summary of electrical parameters found from the dielectric material characterization of the proposed paper substrates. It can be seen that the paper substrate material shows efficiently low dielectric permittivity values. The S1, S2 and S3 substrates show permittivity values of 1.81, 1.63 and 1.84 along with loss tangents of 0.053, 0.046 and 0.057 respectively. The available substrate heights for the three substrates are also listed in Table 1.

3. Simulation Designs

Using the electrical properties measured by material characterization reflectarray unit elements were modelled in CST Microwave Studio. The modelling was done by considering the element placed inside a waveguide aperture, where they are illuminated by exciting the waveguide cavity with aplane wave of TE_{10} mode, in order to determine the scattering parameters of the element [20]. The conducting walls of the waveguide act as a mirror to electromagnetic fields and it is assumed that element suffers from the same conditions of mutual coupling effects as in a real infinite periodic array. Figure 3 shows the simulated model and the applied boundary conditions used in CST MWS.

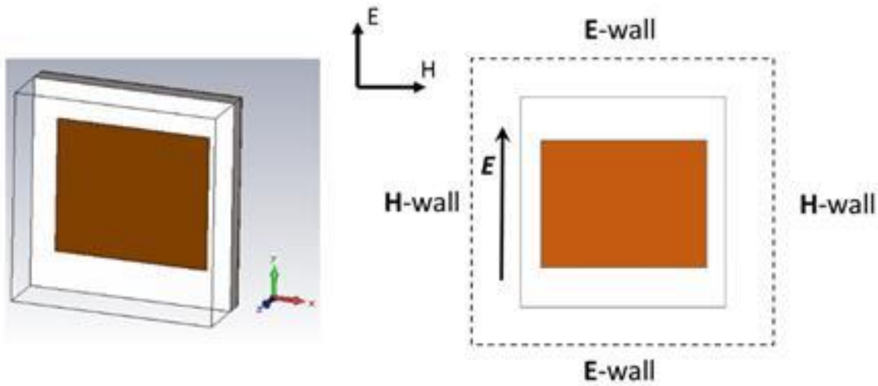

Figure 3. Computer simulated models of rectangular patch element on paper substrates using closed boundary conditions

Simulations were carried out for all the three substrate materials. In order to analyse the behaviour of an infinite reflectarray, the electric and magnetic walls were defined. The vertical walls were nominated as magnetic boundaries while the horizontal walls were nominated as electric boundaries. The vector depicts vertical mode excitation of the simulated patch design. Simulated scattering parameter results in term of reflection phase and reflection loss were analyzed to identify element behavior over the X–band frequency range.

4. Fabrication and Measureements

After simulation and modelling of reflectarray unit elements on paper substrate materials, the elements were fabricated. The fabrication was done using a 70 µm commercially available adhesive copper tape. The simulated designs were first printed over a translucent paper using a laser printer and then the designs were cut into the copper tape manually. The dimensions were carefully monitored for any dimensional tolerances and the technique was fairly improved by fabricating multiple samples. Finally, the elements were then measured for tolerances to avoid any fabrication errors. Multiple elements were fabricated and tested to ensure repeatability of the results. Figure 4 shows the fabricated rectangular patch elements along with the measurement set-up used for the scattering parameter measurements.

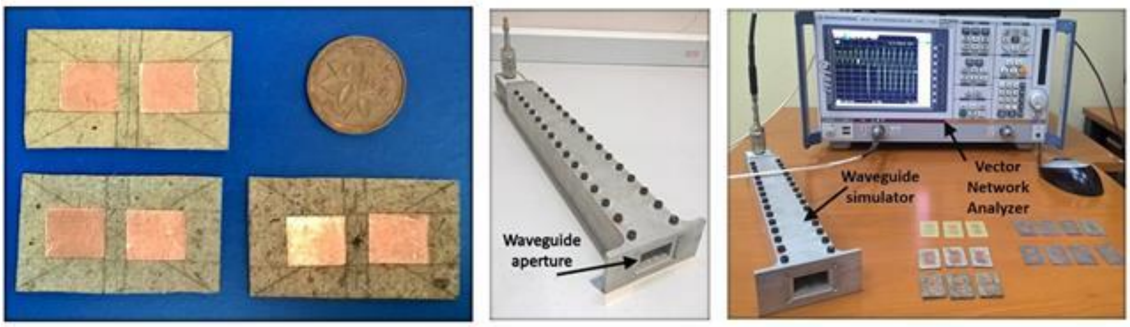

(a) (b) (c)

Figure 4. Scattering parameter measurements (a) Fabricated elements (b) Waveguide simulator (c) Full measurement set-up

Measurement set-up for scattering parameters is shown in Figure 4 (c). An X-band tapered waveguide simulator was used for measurements as depictied in Figure 4 (b). The waveguide connected to a Rodhe & Schwarz 14 GHz vector network analyser for scattering parameter measurements is shown in Figure 4 (c). The elements were placed inside the aperture of the waveguide to measure the scattering parameter results.

5. Results and Analysis

The measurement results for the three substrate materials with a rectangular patch as a radiating element have been plotted and analysed. Performance comparison of proposed three substrates has been carried out on the basis of 10% bandwidth, reflection loss, phase range and slope of the phase curve. Figure 5 (a) shows the measured and the simulated results of scattering parameters. The results show a good agreement between the measured and the simulated results. The reflection loss curves show ripples in curves, these ripples are due to non-ideal nature of waveguide simulator. Figure 5 (b) shows the reflection phase curves of simulated and fabricated samples. The curves follow a gradual decreasing trend with a maximum slope at the resonance point. In order to compare the gradient of the reflection phase curve with the available bandwidth, a Figure of Merit (FOM) has been defined as:

$$FOM = \frac{\Delta\varphi}{\Delta f} \text{ º/MHz}$$

Where $\Delta\varphi$ represents the linear static phase region of the phase curve where the phase remains linear with respect to resonant frequency range of Δf. The 10 % bandwidth is defined by moving 10% above the maximum loss level of a reflection loss curve. A summary of all the findings from Figure 5 are tabulated in Table 2.

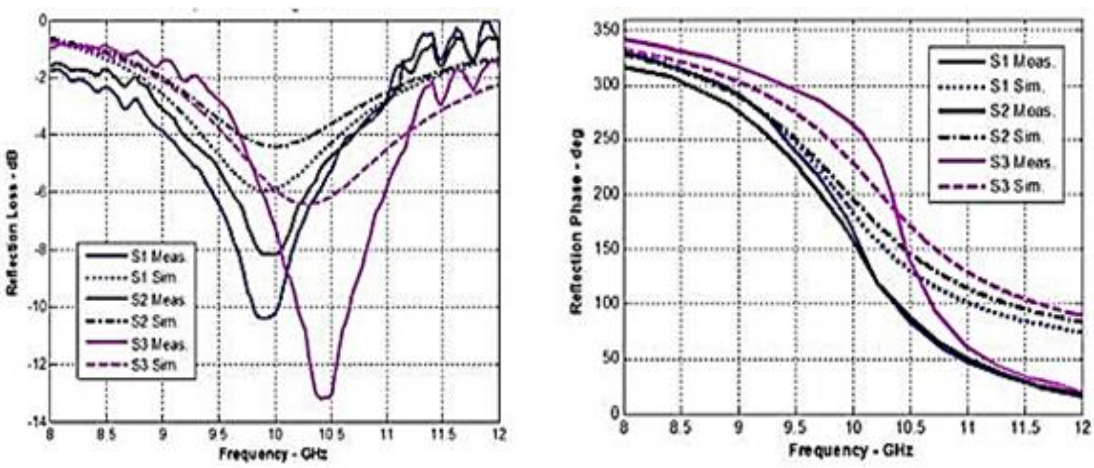

(a) (b)

Figure 5. Comparison between measured and simulated results
(a) reflection loss (b) reflection phase

Table 2. Comparison between Measured and Simulated Scattering Parameters

Substrate (height - mm)		Resonance (GHz)	Reflection Loss (dB)	Bandwidth (MHz) 10%	Phase Range (deg)	FOM (º/MHz)
S1	Sim.	9.92	- 5.92	465	254	0.13
(1.45 mm)	Meas.	9.94	- 10.36	312	308	0.19
S2	Sim.	9.98	- 4.38	682	243	0.10
(1.62 mm)	Meas.	9.95	- 8.16	340	301	0.14
S3	Sim.	10.46	- 6.41	356	275	0.12
(1.12 mm)	Meas.	10.42	-13.19	207	319	0.28

Table 2 highlights the performance comparison of three different substrate materials. The results of scattering parameter measurements show a resonance of 9.94, 9.95 and

10.42 GHz for S1, S2 and S3 substrate materials respectively. The measured loss for three substrates are -10.56, -8.16 and -13.19 dB respectively. In comparison the S3 substrate material shows the maximum loss when compared to other substrates, due to higher loss tangent and a thinner substrate. On the basis of available bandwidth for all the three substrates S2 substrate offers the best bandwidth of 340 MHz followed by 312 and 207 MHz for S1 and S3 substrates respectively. The decrease in the bandwidth of S3 substrate is due to higher reflection loss.

Table 2 also tabulates the reflection phase ranges of the simulated and fabricated designs. For reflectarray unit elements a linear reflection phase of 360º is usually desired to avoid phase error via fabrication tolerances. The proposed elements on broadband paper substrates show measured phase ranges of 308º, 301º and 319º for S1, S2 and S3 substrates respectively. From Table 2, it can also be seen that the phase range for measured results is more than the simulated results. This happens because of the increase in loss of the element. The calculated FOM for the all the three substrates show that the gradient of the phase curve increases with an increased reflection loss. The substrate materials S1, S2 and S3 show measured FOM of 0.19, 0.14 and 0.28 º/MHz respectively. S2 substrate material shows the lowest phase gradient while S3 shows the maximum phase gradient.

The measured results for all the three substrate materials show that the proposed substrate materials show excellent broadband performances. The comparison of the phase ranges and the available bandwidth shows that there is a trade-off between the measured phase range and the available bandwidth. Increased bandwidth does reduces the phase range of the element and vice versa. From the results it can be concluded that the proposed paper substrate materials show promising results in terms of available bandwidth and phase range to help in removing the bandwidth limitation in microstrip reflectarray antennas.

6. Conclusion

In order to address the narrow bandwidth problem in reflectarrays, performance analysis of three different organic substrate materials derived from recycled materials have been carried out. The proposed materials have been characterized for the electrical parameters. The proposed materials show low dielectric permittivity values. Rectangular patch elements were modelled using CST Microwave studio on the proposed substrate materials while taking into considerations the electrical properties of paper substrates. The fabrication was carried out using an Adhesive copper tape method. The fabricated elements were analysed for fabrication tolerances and tested for their scattering parameters using a tapered X-band waveguide simulator. The comparison of measured and simulated results show good agreement along with excellent broadband behaviour with a maximum bandwidth of 340 MHz for S2 substrate material and a good phase range of 301º. Thus it has been demonstrated that proposed paper substrate materials can provide an efficient and a broadband frequency response to overcome the narrow bandwidth drawback in microstrip reflectarray antennas.

References

[1] J Huang. Spacecraft antenna research and development activities aimed at future missions. in *Spaceborne Antennas for Planetary Exploration*, John Wiley & Sons, Inc., 2006: 485–536.

[2] C Tienda, J A Encinar, M Arrebola, M Barba, E Carrasco. Design, manufacturing and test of a dual-reflectarray antenna with improved bandwidth and reduced cross-polarization. *IEEE Trans. Antennas Propag.* 2013; 61(3): 1180–1190.

[3] E Carrasco, J. Perruisseau-Carrier. Reflectarray Antenna at Terahertz Using Graphene. *IEEE Antennas Wirel. Propag. Lett.* 2013; 12: 253–256.

[4] B J Chen, H Yi, K B Ng, S W Qu, C H Chan. *3D printed reflectarray antenna at 60 GHz*. in International Symposium on Antennas and Propagation (ISAP). 2016: 92–93.

[5] M Y. Ismail, M. Inam, *Reflectarray Antennas for Strategic Defense Technology*. Penerbit UTHM, 2012.

[6] T A Metzler. Stub loaded microstrip reflectarrays. in *IEEE Antennas and Propagation Society International Symposium.* 1995; 1: 574–577.

[7] M E Bialkowski, K. H. Sayidmarie. Investigations Into Phase Characteristics of a Single-Layer Reflectarray Employing Patch or Ring Elements of Variable Size. *IEEE Trans. Antennas Propag.* 2008; 56(11): 3366–3372.

[8] B Strassner, C Han, K Chang. Circularly polarized reflectarray with microstrip ring elements having variable rotation angles. *IEEE Trans. Antennas Propag.* 2004; 52(4): 1122–1125.
[9] M Y Ismail, M Inam. Performance improvement of reflectarrays based on embedded slots configurations. *Prog. Electromagn. Res. C*. 2010; 14: 67–78.
[10] H I Malik, M Y Ismail, M Amin, F Mohamed. Design of a Dual C slot Reflectarray with Enhanced Phase Range Performance. *J. Phys. Conf. Ser.* 2017; 852(1): 12034.
[11] T. Isernia and A. F. Morabito, "Mask-Constrained Power Synthesis of Linear Arrays With Even Excitations," *IEEE Trans. Antennas Propag.*, vol. 64, no. 7, pp. 3212–3217, Jul. 2016.
[12] A. F. Morabito and P. G. Nicolaci, "Optimal Synthesis of Shaped Beams Through Concentric Ring Isophoric Sparse Arrays," *IEEE Antennas Wirel. Propag. Lett.* 2017; 16: 979–982.
[13] G. Kumar and K. P. Ray, *Broadband Microstrip Antennas*. Artech House, 2003.
[14] J. A. Encinar *et al.*, "Dual-Polarization Reflectarray in Ku-band Based on Two Layers of Dipole-Arrays for a Transmit-Receive Satellite Antenna with South American Coverage," *2017 11th Eur. Conf. Antennas Propag.* 2017: 80–83.
[15] C. Han, J. Huang, and K. Chang, "A high efficiency offset-fed X/Ka-dual-band reflectarray using thin membranes," *IEEE Trans. Antennas Propag.* 2005; 53(9): 2792–2798.
[16] J. A. Encinar and J. A. Zornoza, "Three-layer printed reflectarrays for contoured beam space applications," *IEEE Trans. Antennas Propag.* 2004; 52(5): 1138–1148.
[17] R. Deng, Y. Mao, S. Xu, and F. Yang, "A Single-Layer Dual-Band Circularly Polarized Reflectarray With High Aperture Efficiency," *IEEE Trans. Antennas Propag.* 2015; 63(7): 3317–3320.
[18] T. Cai, G. M. Wang, and X. F. Zhang, "Compact dual-resonance element with low phase sensitivity for offset reflectarray antennas," *IEEE Antennas Wirel. Propag. Lett.* 2017; 16: 1213–1216
[19] X Xia, Q Wu, H Wang, C Yu, W Hong. Wideband Millimeter-Wave Microstrip Reflectarray Using Dual-Resonance Unit Cells. *IEEE Antennas Wirel. Propag. Lett.* 2017; 16: 4–7.
[20] J Stockmann, R Hodges. The use of waveguide simulators to measure the resonant frequency of ku-band microstrip arrays. in *IEEE Antennas and Propagation Society, AP-S International Symposium (Digest)*. 2005; 1(1): 417–420.